Materials Chemistry and Physics 225 (2019) 55–59

Contents lists available at ScienceDirect

Materials Chemistry and Physics

journal homepage: www.elsevier.com/locate/matchemphys

Structural and optical investigation of brookite TiO_2 thin films grown by atomic layer deposition on Si (111) substrates

Saif M.H. Qaid[a,b,*], Mukhtar Hussain[a], Mahmoud Hezam[c], M.A. Majeed Khan[c], Hamad Albrithen[d,e,f], Hamid M. Ghaithan[a], Abdullah S. Aldwayyan[a,c]

[a] Physics and Astronomy Department, College of Science, King Saud University, Riyadh, Saudi Arabia
[b] Department of Physics, Faculty of Science, Ibb University, Ibb, Yemen
[c] King Abdullah Institute for Nanotechnology, King Saud University, Riyadh, Saudi Arabia
[d] Research Chair for Tribology, Surface and Interface Sciences, Physics and Astronomy Department, College of Science, King Saud University, Riyadh, Saudi Arabia
[e] ARAMCO Laboratory for Applied Sensing Research, King Abdullah Institute for Nanotechnology, King Saud University, Riyadh, Saudi Arabia
[f] National Center for Nanotechnology and Advanced Materials, King Abdulaziz City for Science and Technology, Riyadh, Saudi Arabia

HIGHLIGHTS

- TiO_2 thin films with brookite phase successfully deposited on Si(111) using ALD.
- Correlated Structural and optical properties perceived and studied.
- Reduction of refractive index observed for films with ultra-small thicknesses.

ARTICLE INFO

Keywords:
Thin films
TiO_2
Brookite
Atomic layer deposition
Optical properties

ABSTRACT

In this paper, titanium dioxide (TiO_2) thin films, deposited on single crystal Si (111) substrates under different temperature conditions by Atomic Layer Deposition (ALD), have been systematically studied by X-ray diffraction, photoluminescence spectroscopy and spectroscopic ellipsometry methods. X-ray diffraction analysis showed that the prepared films have a polycrystalline brookite phase over a growth temperature range of (150–300 °C). Increasing the growth temperature resulted in systematic increase of texturing the polycrystalline grains along the (200) direction, with the film at 300 °C having the highest textur along the (200) direction. This was accompanied by improved photoluminescence of the TiO_2 films with the increasing the growth temperature. The improved crystallinity at higher temperatures was also reflected by higher refractive indices, which were deduced from spectroscopic ellipsometry measurements carried out on the grown films.

1. Introduction

In recent years, Titanium oxide (TiO_2) thin films have been widely used in the field of solar cells [1,2], gas sensors [3] and protective coatings [4,5]. TiO_2 is considered as one of the most promising and suitable photocatalytic materials for energy conversion and environmental remediation due to its excellent properties such as non-toxicity and high surface reactivity [6,7] and chemical stability [8,9]. In addition, TiO_2 thin films have been widely studied for optical applications due to its high transparency and a very small absorption coefficient in the visible range [5,10–13]. For example, in dye-sensitized and perovskite solar cells, a compact thin transparent layer of TiO_2 on the conductive glass is essential to prevent the back transfer of electrons between the conductive glass and the hole transport material [5,11–13]. Therefore, it is important to determine the optical and structural properties of grown TiO_2 thin films such as refractive index, extinction coefficient, film thickness and surface roughness. In addition to that, the surface properties of the grown TiO_2 film can have major impacts on subsequently deposited films [14,15]. In this regard, the structural phase and growth direction must be carefully determined for the grown TiO_2 film. A variety of techniques have been used to deposit ultrathin TiO_2 films so far. These include, suspension coating [16], sputtering [17,18], electrochemical deposition [19], pulsed laser deposition (PLD) [20] and atomic layer deposition (ALD) [21–26]. Among these, atomic layer deposition (ALD) is an advanced chemical vapour deposition technique that is capable of producing high quality thin

* Corresponding author. Physics and Astronomy Department, College of Science, King Saud University, Riyadh, Saudi Arabia.
E-mail address: sqaid@ksu.edu.sa (S.M.H. Qaid).

https://doi.org/10.1016/j.matchemphys.2018.12.067
Received 2 February 2018; Received in revised form 14 December 2018; Accepted 23 December 2018
Available online 24 December 2018
0254-0584/

films with excellent atomic level control of layer thickness and uniformity.

TiO_2 can form in three crystalline phases: rutile, anatase and brookite. While rutile is the most stable phase for bulk TiO_2, anatase is more stable for TiO_2 nanostructures. In all cases, the TiO_2 brookite phase is usually difficult to produce. D-H Kim et al. [27] used plasma enhanced ALD to fabricate brookite TiO_2 thin films on (110) yttria-stabilized zirconia (YSZ) substrates. M. Reiners et al. [28] used liquid injection ALD to fabricate TiO_2 thin films with mixed anatase/brookite phases. In this work, and for the first time, we show that TiO_2 thin films with pure brookite phase can be deposited on Si(111) substrates using conventional ALD technique.

2. Experimental details

In the present work, TiO_2 thin films were deposited on Si (111) wafers by atomic layer deposition (ALD) (Beneq TFS 200). The Si wafers were cleaned prior to deposition using ethanol and acetone in an ultrasonic bath for ~30 min. Film deposition was carried out under different temperature of 150 °C, 200 °C, 250 °C, and 300 °C and a base pressure of ~17 mbar. Titanium tetrachloride ($TiCl_4$) and deionized water were used as precursors for the deposition process. The evaporation temperature of $TiCl_4$ was kept at 25 °C while it was 20 °C for deionized water. High purity (99.9999%) nitrogen gas was used as a purging and carrying gas. The flow rates of the carrier gas through $TiCl_4$ and deionized water were kept at 150 and 200 standard cubic centimeters/minute (sccm) respectively, and their pressures were respectively kept at 9 mbar and 8 mbar. For each deposition process, successive purge cycles of reaction precursors ($TiCl_4$ and de-ionized water) were performed, while keeping the Si substrate at the required growth temperature. Each cycle consists of two half-cycles; in the first half, $TiCl_4$ vapour pulse is injected to the reaction chamber by the nitrogen carrier gas until self-terminating reactions occur on the substrate. The non-reacted reactants along with the reaction by-products are purged out from the chamber. In the other half cycle, a pulse of deionized water is brought to the reaction chamber, which chemically reacts with the substrate in a self-terminating manner as well. Dry pulses of nitrogen intervene between $TiCl_4$ and de-ionized water pulses. The pulsing scheme for $TiCl_4/N_2/H_2O/N_2$ gases during one cycle was set with time durations of 0.1s: 3s: 0.1s: 4s. Two sets of samples were prepared. The first set was prepared, using the above-mentioned pulsing scheme, at different growth temperatures of 150 °C, 200 °C, 250 °C and 300 °C using 1000 coating cycles. The second set consists of thin films prepared using the same pulsing scheme at 300 °C but with different thicknesses, which was achieved using different number of coating cycles of 200, 600, 1000 and 1500 cycles.

The structural properties of the grown films were investigated by a Field Emission Scanning Electron Microscope FE-SEM (model: JEOL JSM-7600F) and X-Ray Diffractometer XRD (PANalytical X'pert MPD in the θ-2θ mode. CuKα radiation was used in XRD measurements at 45 kV and 40 mA, and the scanning angle was changed between 2θ = 20° - 50° in steps of 0.01°. Spectroscopic ellipsometry measurements (model: WVASE- J. A. Woolam) were carried out to determine the thickness and optical constants in the wavelength range of 500–2500 nm at an angle of incidence of 50°. The optical constant and the thickness of TiO_2 thin films deposited on Si(111) substrates were fitted using the Cauchy model. Photoluminescence spectra of the films were carried out with a luminescence spectroscopy system (Perkin-Elmer, LS45).

3. Results and discussion

3.1. Structural properties

Fig. 1 shows a cross-sectional image for a film grown at 300 °C using 600 cycles. As expected, the grown film shows a highly uniform thickness of 25 nm over the Si substrate. To determine the crystal

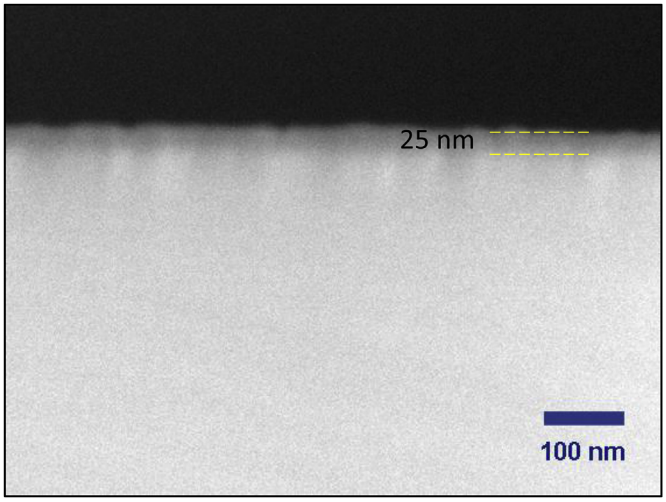

Fig. 1. Cross-sectional FE-SEM image showing the Si/TiO_2 interface.

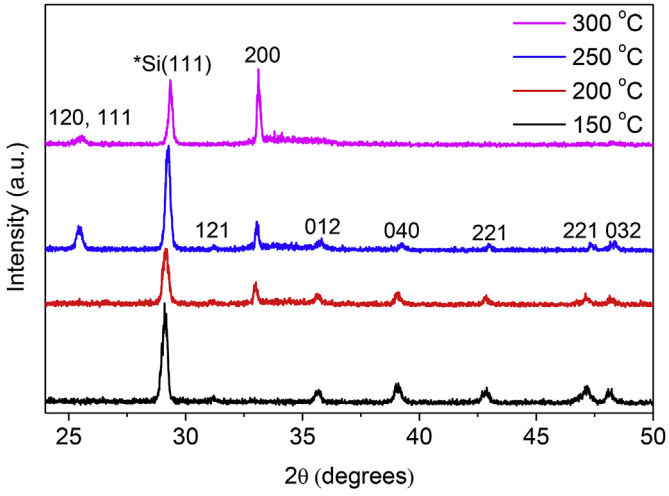

Fig. 2. X-ray diffraction patterns of TiO_2 thin films deposited on Si substrates under different temperatures.

structure and possible phase changes of the films, X-ray analysis was performed. Fig. 2 shows the XRD pattern for the four samples deposited at different temperatures in the range between 150° to 300°. Interestingly, all samples show diffraction peaks that can be well indexed with the crystal structure of the pure brookite phase TiO_2 (JCPDS card no. 29–1360). It can be noticed that the film grown at 150 °C is highly untextured where XRD peaks correspond to different lattice planes in the XRD pattern. When the growth temperature is increased from 150 °C to 300 °C, texture along the (200) direction was observed, and it was improved until almost a full texture along (200) direction is achieved for a growth temperature of 300 °C. This texture improvement explains the strong effect of growth temperature on the structural properties of ALD grown films.

The (200) peak was further analyzed in order to estimate the lattice constant (d_{200}) in the grown films, which can be estimated using Bragg's formula:

$$2\, d_{200}\, sin\theta_{200} = \lambda \quad (1)$$

and the results are shown in Table 1. For the 150 °C sample, the (200) peak was absent, and estimation of d_{200} value could not be performed. For the other samples, it can be noticed that the (200) peak position systematically shifts from 32.99° to 33.13° when the temperature is increased from 200 °C to 300 °C. This implies a contraction behavior of the crystalline lattice, for which the lattice constant of (200) planes

Table 1
Lattice constants of TiO_2 films grown at different growth temperature.

Growth Temperature	$2\theta_{200}$ (degrees)	d_{200} (Å)
150 °C	–	–
200 °C	32.99	2.713
250 °C	33.07	2.707
300 °C	33.13	2.702

(d_{200}) decreased from 2.713 Å at 200 °C to 2.702 Å at 300 °C. This decrease of lattice constant can be explained by the reduced strain at higher growth temperatures [29].

As mentioned above, the rutile and anatase phases are the most stable for TiO_2. The brookite phase is usually more difficult to produce, with different growth models and assumptions regarding how the brookite phase is formed during the growth. For the hydrothermal solution growth of TiO_2, it has been well established that the presence of sodium (Na^+) or other alkali ions has a strong effect on driving the crystallization process into the brookite phase, and there have been different reports proving this fact [30]. For thin films, however, the presence of Na^+ ions is not always available and other growth models have to be proposed. In fact, different thin film deposition techniques were reported to grow brookite TiO_2 films, but in most of them the brookite phase was mixed with rutile/anatase phases. For a pure brookite thin film, D-H Kim et al. reported the epitaxial growth of brookite TiO_2 on yttria-stabilized zirconia (YSZ) substrates by using plasma enhanced ALD. This success is attributed to the small lattice mismatch between YSZ and brookite lattices [27]. Other successful attempts on the epitaxial growth of brookite were also reported using other techniques [31–33]. The question whether non-epitaxial growth of brookite is also possible, which is confirmed by our work for reporting pure brookite films and by many previous articles reporting mixed phases, has been recently studied by J. Haggerty et al. where 95% brookite thin films could be grown on different substrates using pulsed laser deposition (PLD) [34]. Their work confirms a previous report by M. P. Moret et al. who succeeded to grow brookite rich thin films on Si(111) and other substrates using PLD as well [35]. The realization of non-epitaxial growth of brookite was explained by Haggerty et al. to be highly dependent on the processing and structural properties of the films such annealing temperature, film thickness and substrate. There is still no clear answer on how the brookite crystallization is driven by the above parameters [34], and further studies are still required.

3.2. Photoluminescence spectroscopy

Unlike anatase and rutile, brookite has a direct bandgap, and thus emission activity is expected to be higher than anatase and rutile polymorphs because charge carriers do not need additional phonons for the recombination process [36]. Fig. 3 shows fluorescence spectra of brookite TiO2 thin films deposited at different temperature from 150 to 300 °C, using an excitation wavelength of 370 nm. From the fluorescence spectra, two main emission peaks appear at 408 nm and 421 nm, being equivalent to 3.03 eV and 2.94 eV respectively. Considering the brookite bandgap of 3.14 eV [37,38], both peaks lie in the near-band-edge (NBE) region of the brookite phase. These two NBE emission lines at 408 nm and 421 nm could be assigned respectively to band-to-band transition [37,39] and to shallow defect levels in the bandgap [36,40].

It can be noticed that the intensity of the PL emission at the band edge was highly improved when the growth temperature was increased to 300 °C. In addition to that, a broad defect band started to appear (above 450 nm). The two observations clearly indicate that the radiative channels, both NBE and deep level, in the brookite crystal improved with temperature. This can be attributed to the improvement of crystalline structure with annealing. A similar behavior was also

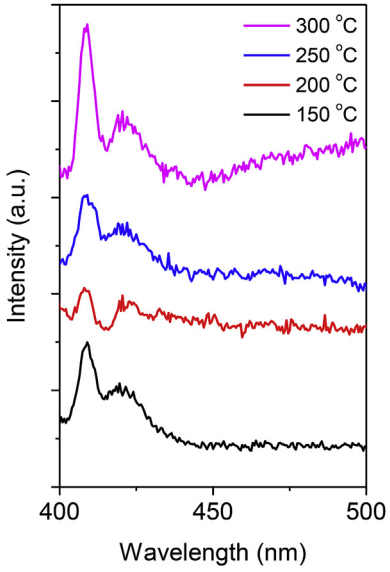

Fig. 3. PL spectra of TiO_2 thin films deposited at different temperatures.

observed by W. F. Zhang et al. [41]. Generally, there are two ways for the relaxation of electrons in the conduction band. The first way is the radiative recombination, either from the band edge or a shallow defect level, to the valence band. The second one is the non-radiative recombination at imperfect lattice points or surface sites. Our results indicate that the radiative recombination channels generally improve when the growth temperature is increased, manifested by improved NBE emission as well as the development of radiative defect emission band at 300 °C.

3.3. Spectroscopic ellipsometry

Spectroscopy ellipsometry is one of the most important characterization optical techniques which is widely used to determine film thickness, refractive index (n), surface and interface roughness of thin films on solid surface. Spectroscopy measurements were carried out using a polarized light with angle of incidence of 50° on the TiO_2 front surface. A three-layer-model was assumed in order to fit the measured ellipsometric constants (Ψ and Δ). Each sample was assumed to consist of Si substrate/a native SiO_2 layer/TiO_2 layer/TiO_2-air mixed layer. The TiO_2-air mixed layer is a virtual optical layer mixed of 50%–50% air and TiO_2, and is proposed to estimate the film roughness. The thickness of the SiO_2 native oxide layer was introduced with a value of 1 nm. The ellipsometry reflection data were collected and fitted, assuming the above-mentioned architecture, using the Cauchy dispersion model [42,43], which is given by:

$$n(\lambda) = A + \frac{B}{\lambda^2} + \frac{C}{\lambda^4} \quad (2)$$

where A, B, and C are Cauchy parameters and λ is the wavelength. Further details on the fitting model along with the best fits to the measured ellipsometric constants Ψ and Δ of all deposited films can be found in the Supplementary Materials (Figs. S1–S3). The thickness and the wavelength-dependent refractive index of TiO_2 thin films deposited on Si substrates could subsequently be extracted from the fitted data.

3.3.1. Effect of growth temperature

The estimated spectral variation of the refractive indices for the TiO_2 thin films deposited at different temperatures is shown in Fig. 4. These results are given within the range of wavelength (500–2500 nm) for ellipsometry measurements as a function of growth temperature. As shown in Fig. 4, for each deposited film, the refractive index is almost invariant in the region from ~1000 to 2500 nm. Below ~1000 nm, the

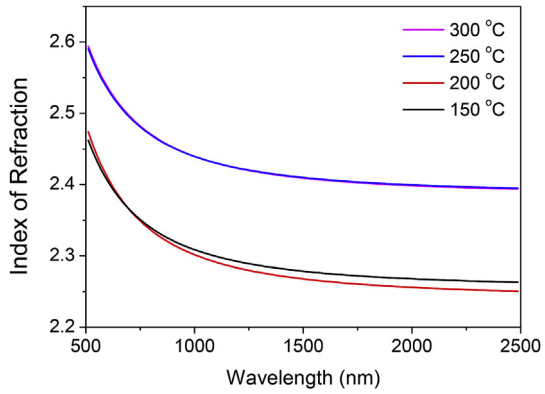

Fig. 4. Refractive indices of brookite TiO_2 thin films (Brookite phase) deposited at different temperatures.

refractive index rapidly decreases with increasing wavelength. Decreasing refractive index with the incident wavelength indicates the normal Cauchy dispersion behavior of the TiO_2 thin films. It can be noticed, however, that the refractive index showed a noticeable increase when the growth temperatures increased to 250 °C and 300 °C. This can be explained by the higher crystalline texture of films grown at higher temperatures, which can modify the refractive index and the reflectivity of the film. In this work, the refractive indices of our TiO_2 thin films deposited at 150 °C, 200 °C, 250 °C and 300 °C were found to be 2.431, 2.444, 2.55 and 2.56 respectively, at the wavelength of 550 nm. Similar results were found by for TiO_2 layers using the atomic layer deposition [44] and by other deposition techniques as well [45,46].

Fig. 5 shows the film thickness as well as the roughness (thickness of the virtual layer) data for deposited films. The film thickness for all films has an average value of 42.75 ± 0.98 nm, which corresponds to a growth rate of 0.43 Å per cycle. The small roughness of ~1 nm in all samples indicates the high level of control offered by ALD over a wide range of growth temperatures. It can be noticed that at 200 °C, the film thickness was noticeably smaller (38.7 nm). It has been reported by other works [47,48] that at a growth temperature of ~200 °C anomalous behaviors and phase transitions occur for TiO_2 grown by ALD. In this work, this effect was greatly eliminated, and only manifested by a small decrease in the overall thickness. The smaller thickness at 200 °C can also explain the reduced PL at 200 °C in Fig. 3.

3.3.2. Effect of ALD cycles

The second set of samples were deposited at a growth temperature of 300 °C using 200, 600, 1000 and 1500 cycles. The accuracy of our ellipsometry analysis can be remarked by the agreement of estimated film thickness at 600 cycles of 24.8 nm with the FE-SEM image in Fig. 1.

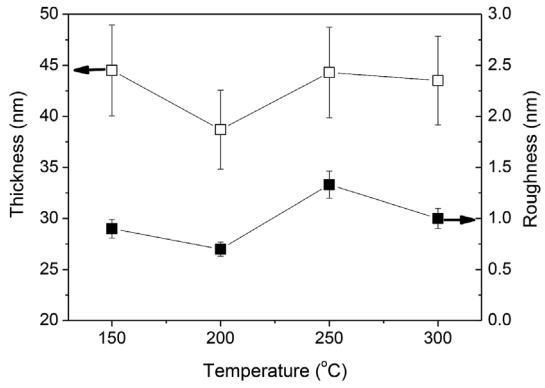

Fig. 5. Thickness and roughness measurements, obtained from the optical spectrometric analysis, for the TiO_2 thin films grown at different temperatures.

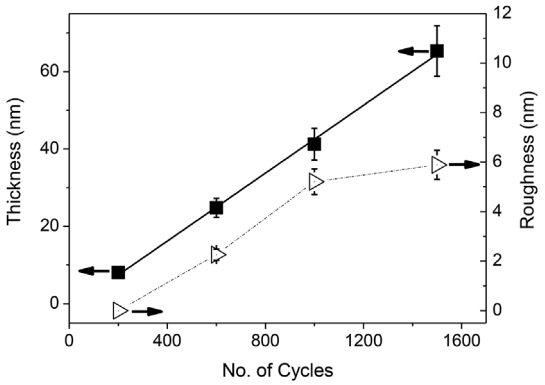

Fig. 6. Dependence of the deposited TiO_2 film thicknesses and surface roughness on coating cycles number at 300 °C.

Fig. 6 shows the film thickness and roughness results as a function of the completed number of coating cycles. We observe the expected linear relation between thickness and number of cycles indicating homogenous growth and linearity effect of the number of cycles on the film thickness. A linear fitting yields a growth rate of 0.44 Å/cycle of the film. Compared to the average growth rate estimated above for samples prepared under different temperatures of 0.43 Å/cycle, it can be concluded that the estimation of film thickness is highly robust and negligibly dependent on the growth temperature. The film roughness is also shown in Fig. 6. Evidently, a systematic increase in the film roughness is observed with increasing the thickness (notice that the roughness at 200 cycles was too small to be detected) until it begins to saturate, at ~ 5–6 nm, above 1000 cycles.

Fig. 7 shows the refractive index of thin films deposited at different coating cycles. It can be noticed that at small number of cycles, the refractive index undergoes a noticeable decrease over the whole wavelength range, in agreement with others' works [49,50]. ALD prepared thin films with ultra-small thicknesses were previously report to show quantum confinement effects [49]. As can be seen in Fig. 6, at 200 cycles, the deposited film has a thickness of ~8 nm, which is within the exciton Bohr radius in semiconducting materials including TiO_2 (1–10 nm) [51]. Therefore, it is likely to observe the quantum size effect in TiO_2 thin films prepared by ALD in similar range of film thickness. However, this conclusion is difficult to be confirmed with the available data especially that the Cauchy model gives no information about the position of the band edge. The sharp decrease in the refractive index can also be correlated to retarded crystallization at very thin layers. At thicknesses below the crystallization threshold, the TiO_2 film can be fully amorphous, resulting in TiO_2 films with lower density and lower refractive index. Additional analysis is still required to undoubtedly explain the reduced refractive index of ultra-thin TiO_2 films.

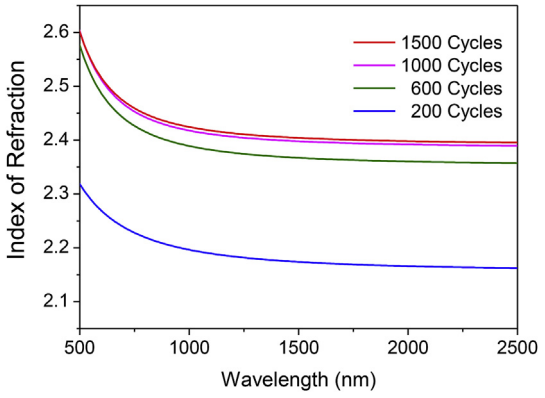

Fig. 7. Refractive index for deposited brookite TiO_2 film at 300 °C using coating cycles of 200, 600, 1000 and 1500 cycles.

4. Conclusion

In conclusion, TiO_2 films were deposited on Si (111) substrates using ALD technique over deposition temperatures range of 150 °C–300 °C. Purity of the brookite phase in all studied samples has been confirmed with XRD measurements. Spectroscopic ellipsometry data measured for these TiO_2 thin films were fitted using the Cauchy model. The refractive index increases with increasing the growth temperature, and a noticeable reduction in the refractive index is observed for ultrathin deposited films using 200–600 coating cycles. PL emission studies showed two peaks in the NBE region, and the emission activity was shown to increase with the growth temperature.

Acknowledgements

The authors thank the Deanship of Scientific Research at King Saud University for funding this work through Research Group No. RG-1440-038.

Appendix A. Supplementary data

Supplementary data to this article can be found online at https://doi.org/10.1016/j.matchemphys.2018.12.067.

References

[1] H.M. Ghaithan, S.M. Qaid, M. Hezam, M.B. Siddique, I.M. Bedja, A.S. Aldwayyana, Invoking the frequency dependence in square modulated light intensity techniques for the measurement of electron time constants in dye-sensitized solar cells, Proc. SPIE-Int. Soc. Opt. Eng. 9556 (2015) 1–8.
[2] H.M. Ghaithan, S.M.H. Qaid, M. Hezam, J.P. Labis, M. Alduraibi, I.M. Bedja, A.S. Aldwayyan, Laser induced photocurrent and photovoltage transient measurements of dye-sensitized solar cells based on TiO2 nanosheets and TiO2 nanoparticles, Electrochim. Acta 212 (2016) 992–997.
[3] S.R. Morrison, Selectivity in semiconductor gas sensors, Sensor. Actuator. 12 (1987) 425–440.
[4] F. Mansfeld, Models for the impedance behavior of protective coatings and cases of localized corrosion, Electrochim. Acta 38 (1993) 1891–1897.
[5] X. Feng, K. Shankar, O.K. Varghese, M. Paulose, T.J. Latempa, C.A. Grimes, Vertically aligned single crystal TiO 2 nanowire arrays grown directly on transparent conducting oxide coated glass: synthesis details and applications, Nano Lett. 8 (2008) 3781–3786.
[6] U. Diebold, The surface science of titanium dioxide, Surf. Sci. Rep. 48 (2003) 53–229.
[7] Z.X. Xiguang Han, Kuang Qin, Jin Mingshang, Synthesis of titania nanosheets with a high percentage of exposed (001) facets facets and related photocatalytic properties, Am. Chem. Soc. (2009) 3152–3153.
[8] H.G. Yang, C.H. Sun, S.Z. Qiao, J. Zou, G. Liu, S.C. Smith, H.M. Cheng, G.Q. Lu, Anatase TiO2 single crystals with a large percentage of reactive facets, Nature 453 (2008) 638–641.
[9] J. Zhang, Q. Xu, Z. Feng, M. Li, C. Li, Importance of the relationship between surface phases and photocatalytic activity of TiO2, Angew. Chem. Int. Ed. 47 (2008) 1766–1769.
[10] S. Pang, H. Hu, J. Zhang, S. Lv, Y. Yu, F. Wei, T. Qin, H. Xu, Z. Liu, G. Cui, NH2CH = NH2PbI3: an alternative organolead iodide perovskite sensitizer for mesoscopic solar cells, Chem. Mater. 26 (2014) 1485–1491.
[11] H. Choi, C. Nahm, J. Kim, J. Moon, S. Nam, D.R. Jung, B. Park, The effect of TiCl 4-treated TiO 2 compact layer on the performance of dye-sensitized solar cell, Curr. Appl. Phys. 12 (2012) 737–741.
[12] P. Lellig, Application of a Hybrid Blocking Layer in Dye-sensitized Solar Cells Dissertation, (2011).
[13] L. Meng, C. Li, Blocking layer effect on dye-sensitized solar cells assembled with TiO (2) nanorods prepared by dc reactive magnetron sputtering, Nanosci. Nanotechnol. Lett. 3 (2011) 181–185.
[14] E. Mosconi, E. Ronca, F. De Angelis, First-principles investigation of the TiO 2/Organohalide perovskites interface: the role of interfacial chlorine, J. Phys. Chem. Lett. 5 (2014) 2619–2625.
[15] A. Kogo, Y. Sanehira, M. Ikegami, T. Miyasaka, Brookite TiO 2 as a low-temperature solution-processed mesoporous layer for hybrid perovskite solar cells, J. Mater. Chem. A. 3 (2015) 20952–20957.
[16] J. Liu, Y. Nakamura, T. Ogura, Y. Shibasaki, S. Ando, M. Ueda, Optically transparent sulfur-containing Polyimide – TiO 2 nanocomposite films with high refractive index and negative pattern formation from poly(amic acid) – TiO 2 nanocomposite film, Chem. Mater. 20 (2008) 273–281.
[17] H.I. Elim, B. Cai, Y. Kurata, O. Sugihara, T. Kaino, T. Adschiri, A.-L. Chu, N. Kambe, Refractive index control and Rayleigh scattering properties of transparent TiO 2 nanohybrid polymer, J. Phys. Chem. B 113 (2009) 10143–10148.
[18] D. Rafieian, W. Ogieglo, T. Savenije, R.G.H. Lammertink, Controlled formation of anatase and rutile TiO 2 thin films by reactive magnetron sputtering, AIP Adv. 5 (2015) 097168.
[19] A. Visan, D. Rafieian, W. Ogieglo, R.G.H. Lammertink, Modeling intrinsic kinetics in immobilized photocatalytic microreactors, Appl. Catal. B Environ. 150 (2014) 93–100.
[20] M. Horprathum, P. Eiamchai, P. Limnonthakul, N. Nuntawong, P. Chindaudom, A. Pokaipisit, P. Limsuwan, Structural, optical and hydrophilic properties of nanocrystalline TiO2 ultra-thin films prepared by pulsed dc reactive magnetron sputtering, J. Alloy. Comp. 509 (2011) 4520–4524.
[21] A. Manivannan, N. Spataru, K. Arihara, A. Fujishima, Electrochemical deposition of titanium oxide on boron-doped diamond electrodes, Electrochem. Solid State Lett. 8 (2005) C138.
[22] M.M. Shirolkar, D. Phase, V. Sathe, J. Rodríguez-Carvajal, R.J. Choudhary, S.K. Kulkarni, Relation between crystallinity and chemical nature of surface on wettability: a study on pulsed laser deposited TiO 2 thin films, J. Appl. Phys. 109 (2011) 123512.
[23] J. Alam, M. Alhoshan, L.A. Dass, A.K. Shukla, M.R. Muthumareeswaran, M. Hussain, A.S. Aldwayyan, Atomic layer deposition of TiO2 film on a polyethersulfone membrane: separation applications, J. Polym. Res. 23 (2016) 183.
[24] J. Aarik, H. Mändar, M. Kirm, L. Pung, Optical characterization of HfO2 thin films grown by atomic layer deposition, Thin Solid Films 466 (2004) 41–47.
[25] M. Leskelä, M. Ritala, Atomic layer deposition (ALD): from precursors to thin film structures, Thin Solid Films 409 (2002) 138–146.
[26] A. Suisalu, J. Aarik, H. Mändar, I. Sildos, Spectroscopic study of nanocrystalline TiO2 thin films grown by atomic layer deposition, Thin Solid Films 336 (1998) 295–298.
[27] D.H. Kim, W.S. Kim, S. Kim, S.H. Hong, Brookite TiO2 thin film epitaxially grown on (110) YSZ substrate by atomic layer deposition, ACS Appl. Mater. Interfaces 6 (2014) 11817–11822.
[28] M. Reiners, K. Xu, N. Aslam, A. Devi, R. Waser, S. Hoffmann-Eifert, Growth and crystallization of TiO 2 thin films by atomic layer deposition using a novel amido guanidinate titanium source and tetrakis-dimethylamido-titanium, Chem. Mater. 25 (2013) 2934–2943.
[29] S.C. Seel, C.V. Thompson, S.J. Hearne, J. a. Floro, Tensile stress evolution during deposition of Volmer–Weber thin films, J. Appl. Phys. 88 (2000) 7079.
[30] M. Cargnello, T.R. Gordon, C.B. Murray, Solution-phase synthesis of titanium dioxide nanoparticles and nanocrystals, Chem. Rev. 114 (2014) 9319–9345.
[31] K.M.K. Srivatsa, M. Bera, A. Basu, Pure brookite titania crystals with large surface area deposited by Plasma Enhanced Chemical Vapour Deposition technique, Thin Solid Films 516 (2008) 7443–7446.
[32] M.G. Manera, A. Taurino, M. Catalano, R. Rella, A.P. Caricato, R. Buonsanti, P.D. Cozzoli, M. Martino, Enhancement of the optically activated NO2gas sensing response of brookite TiO2nanorods/nanoparticles thin films deposited by matrix-assisted pulsed-laser evaporation, Sensor. Actuator. B Chem. 161 (2012) 869–879.
[33] W. Wang, M. Wang, Z. Li, X. Du, H. Xu, W. Zhao, X. Feng, J. Ma, Synthesis and characterization of structural and optical properties of heteroepitaxial brookite TiO2single crystalline films, Scripta Mater. 115 (2016) 75–79.
[34] J.E.S. Haggerty, L.T. Schelhas, D.A. Kitchaev, J.S. Mangum, L.M. Garten, W. Sun, K.H. Stone, J.D. Perkins, M.F. Toney, G. Ceder, D.S. Ginley, B.P. Gorman, J. Tate, High-fraction brookite films from amorphous precursors, Sci. Rep. 7 (2017) 1–11.
[35] M.P. Moret, R. Zallen, D.P. Vijay, S.B. Desu, Brookite-rich titania films made by pulsed laser deposition, Thin Solid Films 366 (2000) 8–10.
[36] J. Zhang, P. Zhou, J. Liu, J. Yu, New understanding of the difference of photocatalytic activity among anatase, rutile and brookite TiO2, Phys. Chem. Chem. Phys. 16 (2014) 20382–20386.
[37] G. Zhu, T. Lin, X. Lü, W. Zhao, C. Yang, Z. Wang, H. Yin, Z. Liu, F. Huang, J. Lin, Black brookite titania with high solar absorption and excellent photocatalytic performance, J. Mater. Chem. A. 1 (2013) 9650–9653.
[38] D. Reyes-Coronado, G. Rodr??guez-Gattorno, M.E. Espinosa-Pesqueira, C. Cab, R. De Coss, G. Oskam, Phase-pure TiO2 nanoparticles: anatase, brookite and rutile, Nanotechnology 19 (2008).
[39] E.D. Yu, H.H. Yu, D.S. Zhou, L.D. JIANG, D.S, GU, Structural phase transition and photoluminescence of TiO_2 nano-crystals, Chin. J. Lumin. 27 (2) (2006) 239.
[40] D.K. Pallotti, L. Passoni, P. Maddalena, F. Di Fonzo, S. Lettieri, Photoluminescence mechanisms in anatase and rutile TiO2, J. Phys. Chem. C 121 (2017) 9011–9021.
[41] W.F. Zhang, M.S. Zhang, Z. Yin, Microstructures and visible photoluminescence of TiO2 nanocrystals, Phys. Status Solidi Appl. Res. 179 (2000) 319–327.
[42] R. Synowicki, Spectroscopic ellipsometry characterization of indium tin oxide film microstructure and optical constants, Thin Solid Films 313 (1998) 394–397.
[43] M. Rebien, W. Henrion, M. Hong, J.P. Mannaerts, M. Fleischer, Optical Properties of Gallium Oxide Thin Films, (n.d.).
[44] M.-L. Kääriäinen, D.C. Cameron, The Importance of the Majority Carrier Polarity and P-n Junction in Titanium Dioxide Films to Their Photoactivity and Photocatalytic Properties, (2012).
[45] P. Eiamchai, P. Chindaudom, A. Pokaipisit, P. Limsuwan, A spectroscopic ellipsometry study of TiO2 thin films prepared by ion-assisted electron-beam evaporation, Curr. Appl. Phys. 9 (2009) 707–712.
[46] M. Kang, S.W. Kim, H.Y. Park, Optical properties of TiO2 thin films with crystal structure, J. Phys. Chem. Solid. 123 (2018) 266–270.
[47] J. Aarik, A. Aidla, H. Mandar, V. Sammelselg, Anomalous effect of temperature on atomic layer deposition of titanium dioxide, J. Cryst. Growth 220 (2000) 531–537.
[48] J. Leem, I. Park, Y. Li, W. Zhou, Z. Jin, S. Shin, Y. Min, Role of HCl in atomic layer deposition of TiO2 thin films from titanium tetrachloride and water, Bull. Korean Chem. Soc. 35 (2014) 1195–1201.
[49] D.M. King, X. Du, A.S. Cavanagh, A.W. Weimer, Quantum confinement in amorphous TiO(2) films studied via atomic layer deposition, Nanotechnology 19 (2008) 445401.
[50] G. Triani, J.A. Campbell, P.J. Evans, J. Davis, B.A. Latella, R.P. Burford, Low temperature atomic layer deposition of titania thin films, Thin Solid Films 518 (2010) 3182–3189.
[51] Y.L, R.O. Claus, Blue light emitting nanosized TiO2 colloids, J. Am. Chem. Soc. 119 (22) (1997) 5273–5274.